



A02-13985

AIAA-2002-0485

## Transport Physics in Hall Plasma Thrusters

M. A. Cappelli, N. B. Meezan and N. Gascon

Mechanical Engineering Department

Stanford University

Stanford, CA

**40<sup>th</sup> AIAA Aerospace Sciences Meeting  
and Exhibit**  
14-17 January 2002  
Reno, Nevada

# Transport Physics in Hall Plasma Thrusters

Mark A. Cappelli<sup>†</sup>, Nathan B. Meezan<sup>‡</sup> and N. Gascon<sup>#</sup>

*Mechanical Engineering Department, Stanford University, Stanford, California 94305-3032*

An analysis of measurements supporting the presence of anomalous cross-field electron mobility in Hall plasma accelerators is presented. Non-intrusive laser-induced fluorescence measurements of neutral and ionized xenon velocities, and various electrostatic probe diagnostic measurements are used to locally determine the effective electron Hall parameter inside the accelerator channel. These values are then compared to the classical (collision-driven) Hall parameters expected for a quiescent magnetized plasma. The results indicate that in the vicinity of the anode the electron transport mechanism is consistent with that determined by elastic collisions with the background neutral xenon. However, we find that in the vicinity of the discharge channel exit, where the magnetic field is the strongest and where there are intense fluctuations in the plasma properties, the inferred Hall parameter departs from the classical value, and is close to the Bohm value of  $(\omega_{ce}\tau)_{\text{eff}} \approx 16$ . An exception to this is at the higher values of discharge voltage, where, in regions where there appears to be strong electron azimuthal shear, the value approaches that determined by classical scattering. The spatial variation in the mobility is consistent with that determined from an analysis of turbulent fluctuations in the electron density, and is found to be described by an empirical model that includes the possible effects of azimuthal electron shear in suppressing fluctuations-enhanced electron transport.

## I. INTRODUCTION

The use of coaxial Hall discharges as high specific impulse plasma accelerators for satellite propulsion date back to the early 1960's. In a Hall discharge, the plasma is sustained in imposed orthogonal electric and magnetic fields. The discharge electrons, a large fraction of which are emitted by an external cathode, are magnetized, whereas the more massive propellant ions, usually xenon, are not. Consequently, the electrostatic fields established by the retarded electron flow accelerate the ions to high velocities, typically 50-60% of the discharge voltage. In a co-axial geometry, the electrons are constrained to move in the closed, azimuthal  $E \times B$  drift, with cross-field diffusion providing the necessary current to sustain the discharge.

The first detailed investigation of the properties of these coaxial Hall discharges suggested that the axial electron current density is greater than that expected by classical transport [1]. This led to the first speculation of the presence of an "anomalous" cross-field drift of electrons, due in part to fluctuations in the electric field and plasma density. Fluctuations in the external circuit and plasma properties in these devices are now well documented [2-5], and recent numerical simulations of Hall discharges generally require the *ad hoc* introduction of an anomalous electron mobility to produce reasonably accurate results [6-9]. Despite many experimental and theoretical studies, the precise nature of the instabilities

responsible for these fluctuations and the mechanism for their excitation are not yet well understood. Furthermore, other mechanisms, including collisions between energetic electrons and the channel wall, and experimental facility effects such as background gas ingestion may also play important roles in electron transport.

In this paper, we examine the electron transport mechanism in a coaxial Hall discharge through a collection of applied diagnostics that serve to map the electron mobility in the discharge channel. The 2-D electron momentum equation for a weakly ionized plasma gives the electron current density,

$$J_{ez} = en_e u_{ez} = \frac{v_{ne}^2}{v_{ne}^2 + \omega_{ce}^2} \left( \frac{n_e e^2}{m_e v_{ne}} \right) E_z. \quad (1)$$

Here,  $n_e$  is the electron density,  $u_{ez}$  is the electron drift velocity,  $v_{ne}$  is the momentum-transfer collision frequency for neutral-electron collisions. When the electron cyclotron frequency  $\omega_{ce} \propto v_{ne}$ , this expression reduces to

$$J_{ez} = en_e \left( \frac{E_z}{B_r} \right) \frac{v_{ne}}{\omega_{ce}} = en_e \left( \frac{E_z}{B_r} \right) \frac{1}{\omega_{ce} \tau}, \quad (2)$$

where  $\tau$  is the mean time between collisions and it is assumed that the applied electric field,  $E_z$ , and magnetic field strength,  $B_r$ , are in the axial and radial directions, respectively. From Eqn. 2, we see that the cross-field

<sup>†</sup> Associate Professor, Member AIAA

<sup>‡</sup> Graduate Research Assistant, Student Member, AIAA

<sup>#</sup> Post-doctoral Research Associate, Student Member, AIAA

Copyright© 2002 by Stanford University. Published by the American Institute of Aeronautics and Astronautics, with permission.

electron mobility is inversely proportional to the electron Hall parameter,  $\omega_{ce}\tau$ ,

$$\mu_{ez} = \left( \frac{1}{B_r} \right) \frac{1}{\omega_{ce}\tau}. \quad (3)$$

Equation 2 can be rearranged to give

$$\frac{1}{(\omega_{ce}\tau)} = \left( \frac{B_r}{E_z} \right) \frac{J_{ez}}{en_e}. \quad (4)$$

The electron mobility can therefore be determined at any point in the discharge channel where the plasma properties on the right-hand side of Eqn. 4 are known. Furthermore, the resulting Hall parameter can be compared to that calculated on the basis of known properties that independently determine the electron cyclotron frequency and the mean time between electron collisions.

In this paper, we briefly review the results of our experimental measurements of plasma properties within the discharge channel, which permit this direct comparison. The results support the presence of an anomalous transport mechanism in regions of the plasma known to support fluctuations, and provide the first direct quantitative measure of the axial variation in the electron mobility. Independent experimental values of the mobility are extracted from fluctuations in the electron density measured using the saturated ion current from immersed Langmuir probes. Both measurements point towards the existence of a localized region near the exit plane at which the inverse Hall parameter falls from a value close to that determined from anomalous Bohm transport, to values very close to those determined by classical electron scattering. A remarkable agreement between the two (qualitative and quantitative) lend credence to fluctuations as the anomalous transport mechanism, though ongoing research is focusing on how wall effects might alter the turbulent nature of these magnetized discharges.

## II. EXPERIMENTS

### A. Prototype Hall discharge

The Hall plasma source studied here was constructed at Stanford as a test bed for studying the discharge physics and is not intended to serve as an operational prototype plasma accelerator. A cutaway schematic of the plasma source is shown in Fig. 1. The source consists of an annular alumina channel 90 mm in diameter, 11 mm in width, and 80 mm in length. A magnetic circuit consisting of four outer coils, one inner coil, and three iron plates provides a magnetic field (mostly radial in direction) peaked near the exit of the discharge channel. A hollow stainless steel ring with 32 holes of 0.5 mm diameter serves both as the anode and the propellant (gas) input of the discharge.

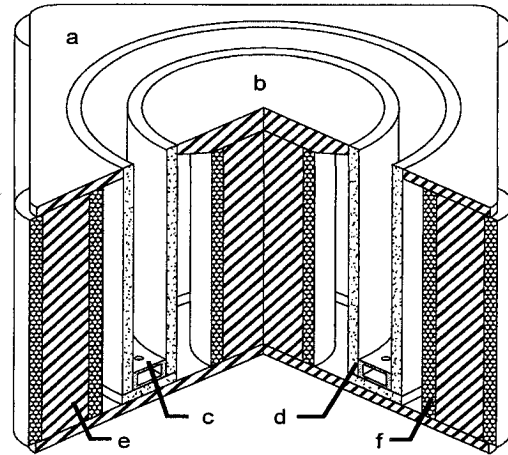


FIG. 1. Cutaway schematic of the Hall discharge studied. a) front magnetic plate b) central magnetic plate c) anode/gas input d) alumina insulator wall e) magnet core f) magnetic windings.

A hollow cathode, needed to neutralize the ion beam and support the electric field, is mounted 2 cm downstream of the plasma source exit. The cathode body was kept at the vacuum chamber ground potential. To allow optical and probe access inside the discharge channel, a 1 mm wide slot was cut along the outer insulator wall, parallel to the discharge axis. The performance of the discharge is not noticeably altered by the presence of the slot.

The experimental facility consists of a non-magnetic stainless steel tank approximately 1 m in diameter and 1.5 m in length pumped by two 50 cm diameter diffusion pumps and backed by a 425 L/sec mechanical pump. The facility is equipped with several viewports and feedthroughs for optical and probe access to the discharge. The base pressure of the facility with no gas flow is approximately  $10^{-6}$  Torr as measured by an ionization gauge uncorrected for gas species. The background pressure during discharge operation at a xenon flow rate of 2.3 mg/s is typically  $10^{-4}$  Torr. Although this pressure is an order of magnitude lower than that of Janes and Lowder [1], it is still considerably higher than chamber pressures that are generally acceptable for the collection of accelerator performance data [10-11]. The ingestion of background gas near the exit of the discharge channel may influence the discharge characteristics.

### B. Plasma Diagnostic Techniques

A variety of optical and probe diagnostics were utilized to measure the plasma properties needed for the determination of the effective Hall parameter (using Eqn. 4). The potential distribution in the discharge was measured using an emissive probe, described in more detail in another paper [12]. The probe consisted of a tungsten filament inserted into the discharge channel, heated using a transformer-coupled, variable-current AC

power supply. The filament current was increased until the potential of the floating transformer with respect to ground reached a nearly saturated value. This value was taken as the plasma potential [13]. The floating potential of the plasma was also recorded at each point using the same probe without current passing through the filament. The magnetic field distribution inside the channel was measured with the discharge off using a Hall-effect sensor probe.

The electron current density is determined from the total discharge current density (discharge current divided by the channel cross sectional area) less the ion current density,

$$J_e = I / A_{channel} - n_e V_i. \quad (5)$$

The ion current density is determined either directly using a guarded ion flux probe, or from a measurement of the electron (ion) density using a cylindrical Langmuir probe and from laser-induced fluorescence (LIF) measurements of the xenon ion velocity. The ion density and electron density are assumed to be equal through the condition of quasi-neutrality. The LIF velocimetry measurements are described in detail elsewhere [12, 14]. They involve propagating a narrow-linewidth, continuous-wave laser beam through the plasma along the discharge axis and measuring the fluorescence signal as a function of laser frequency. Due to the Doppler effect, the absorption line-center is shifted from that of a stationary plasma reference. The bulk velocity of the absorbing xenon ions can then be determined from this frequency shift. In the studies reported here, a tunable titanium sapphire laser was used to excite the  $5d[4]_{7/2} - 6p[3]_{5/2}$  transition in Xe

II at 834.7 nm, with non-resonance fluorescence detected at 541.9 nm. A similar method was also used to measure the velocity of excited neutral xenon atoms using the

$6s\left[\frac{3}{2}\right]_2^o - 6p\left[\frac{3}{2}\right]_2$  transition at 823.2 nm, only in this case,

resonance fluorescence is detected. The neutral atom velocity together with the overall xenon mass flow rate served to provide a measure of the neutral xenon number density, from which the classical Hall parameter can be determined.

Plasma density fluctuations were detected by low-impedance Langmuir probes biased negatively with respect to the plasma potential to collect the ion saturation current [15]. In previous studies of low-frequency fluctuations in current collected from similar probes in Hall discharges, these fluctuations were seen to be largely isothermal [16]. The probe size was minimized so as to reduce its overall capacitance, and for the studies reported on here, was approximately 10 cm in length. The frequency response of the probe was found to be excellent (gain equal to one, no phase shift, within measuring device accuracy) up to 1 MHz, the 3 dB cutoff being at

4MHz. Coaxial transmission line feed-throughs provided the transfer of the probe signal through the vacuum chamber to a digital oscilloscope card operating at an 800 kHz sample rate. The probes were terminated with 50 W at the input of the oscilloscope. In this way, the probe tips were negatively biased (close to system ground) with respect to the plasma, which is predominantly at high positive potential, since the anode is maintained at a minimum of 86V, and since the near exit plane potential is always greater than 40V due to the cathode fall and finite electron temperature. Occasional scans of the Langmuir probe across the electron retarding regime to regions of high negative bias verified that system ground potential was always in the ion current saturation regime. In most cases, the axial probe locations varied between a distance of 45 mm from the anode ( $z = 45$  mm) and 10 mm beyond the exit plane ( $z = 10$  mm), with the  $z = 0$  reference taken to be the exit plane of the discharge, and negative positions implying that the probe locations are inside the discharge channel.

### III. RESULTS AND ANALYSIS

The electric field inside the discharge channel was calculated from the plasma potential data (see Fig. 2) using the relation  $E_z = -d\phi/dz$ . Smooth curves were fit to the potential profiles before differentiation to prevent noise amplification. The plasma potential data was also used in conjunction with floating potential data to calculate the electron temperature:

$$\phi_p - \phi_f = \frac{kT_e}{2e} \ln\left(\frac{m_i}{2\pi m_e}\right). \quad (6)$$

Here, we assume that the ions enter the sheath at the Bohm velocity.

The electron temperature is shown in Fig. 3. These temperature profiles are used in the remaining calculations needed to estimate the Hall parameter. The electron temperature is seen to peak at nearly 16 eV, consistent with the measurements of others in similar discharges [17-18]. The peak in the electron temperature is found to be coincident with the peak in the electric and magnetic field, as expected, since the Ohmic dissipation will scale as  $J_{ez}E_z$ . We see an unexpected rise in the electron temperature near the anode for the higher power cases studied, most likely due to the formation of an anode glow region, as the production of electrons is needed in this region to support the higher current densities. These striking distributions suggest that the discharge length is not optimized, and can be shortened to 40 mm for more efficient operation as a plasma accelerator at the higher voltage conditions.

The electron temperature is used to determine the electron (ion) density from the ion saturation current collected with the Langmuir probe discussed above:

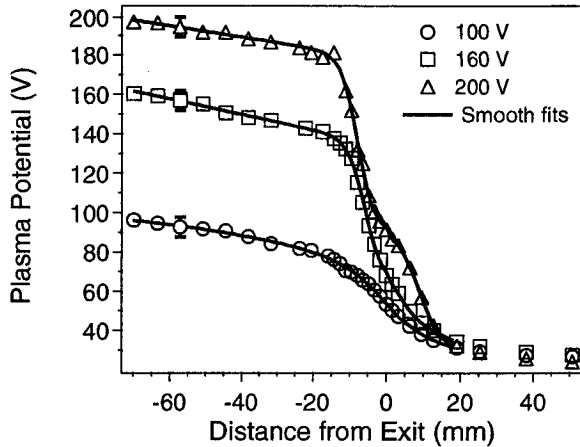


FIG. 2. Plasma potential profiles calculated from emissive probe data.

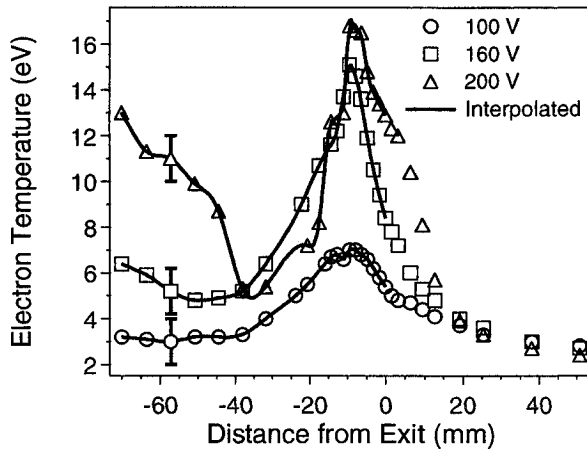


FIG. 3. Electron temperature profiles calculated from plasma and floating potential data.

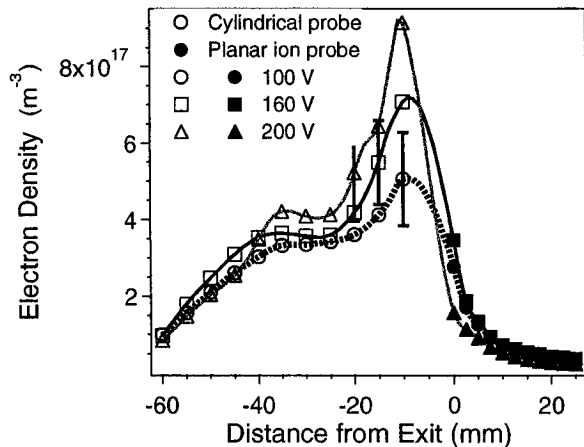


FIG. 4. Electron density profiles from probe experiments.

$$J_{is} = 0.61 en_e \sqrt{\frac{kT_e}{m_i}} \quad (7)$$

The electron density profiles measured from the two probe methods are plotted together in Fig. 4.

The intrusive nature of the guarded ion probe precluded measurements with this probe within the discharge channel. Furthermore, the Langmuir probe inserted through the slot in the insulator was unable to collect data within a distance of 10 mm upstream of the channel exit, because of the presence of the magnetic pole piece. As a result, the two probe measurements were indeed complementary, yet incomplete, and a cubic-spline interpolation was used to estimate the plasma density in the range between the discharge channel exit and the location of the base of the front magnetic plate. The resultant spline fits are also shown in Fig. 4. The electron number densities are seen to peak in the same location where the other plasma properties reach their maximum values.

Knowledge of  $B_r$ ,  $E_z$ ,  $n_e$ , and  $V_i$  (ion velocity) is enough to calculate the effective Hall parameter along the Hall discharge channel from Eqns. 4 and 5. This Hall parameter can be compared to the “classical” Hall parameter expected based on the electron momentum-transfer collision frequency,  $\nu_{en}$ . For this calculation, the neutral gas density (the dominant electron collision partner) is determined from the neutral xenon velocity data and the discharge mass flow rate,

$$n_g = \left( \frac{\dot{m}}{m_i A_{channel}} - n_e V_i \right) \frac{1}{V_n} \quad (8)$$

It is noteworthy that the calculation of the neutral gas density does not take into account ingestion of background gas from the vacuum chamber. Background neutral xenon ingestion would result in an underestimate of the neutral xenon density, as the actual mass flow rate would be higher. The measurements of xenon density use here are interpreted as lower limits of the actual values.

The electron momentum-transfer collision frequency was calculated using the cross-section given in the SIGLO<sup>®</sup> database [19] assuming a Maxwellian electron energy distribution, using the electron temperature measurements described above.

## IV. DISCUSSION

### A. Mobility

The deduced Hall parameter is compared to the “classical” Hall parameter (that determined by the direct calculation of the electron momentum-transfer collision frequency) in Fig. 5. In the figure, the mean time between electron collisions is determined by molecular scattering only (neglect wall scattering), and we plot the inverse of the Hall parameter ( $1/\omega_{ce}\tau$ ), since this is proportional to

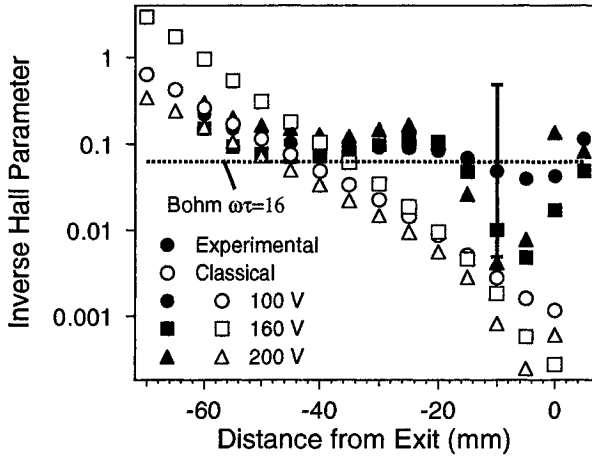


FIG. 5. Effective and classical inverse Hall parameter profiles inside Hall discharge channel.

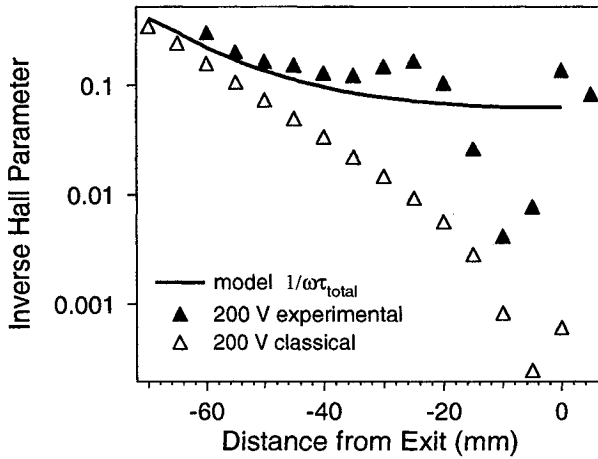


FIG. 6. Comparison of mixed mobility model to experimental and classical inverse Hall parameter profiles at 200 V operation.

the electron cross-field mobility for most of the discharge channel (See Eqn. 2).

It is apparent from Fig. 5 that elastic electron-neutral collisions is the likely mechanism for cross-field electron transport at locations between the anode ( $z = -80$  mm) and approximately 40 mm upstream of the discharge channel exit (although the requirement  $\omega_{ce} \ll \nu_{ne}$  is not satisfied near the anode for the 160V case). We also see that beyond this location, there is a striking departure from this classical value, although the uncertainty in the absolute measurements is still significant, a result mainly attributable to the uncertainty in the total discharge current caused by the intrusive nature of the diagnostic probes. At locations downstream of the  $z = -40$  mm position, where the magnetic field reaches a maximum, the inverse Hall parameter is in remarkable agreement with the Bohm value of  $\omega_{ce}\tau = 16$  [20]. In this region, we

[21-23], and others [2-5, 24-25] have reported on the existence of intense fluctuations in the plasma properties. These results are supportive of the conjecture that plasma fluctuations are partially responsible for the anomalous cross-field transport, although additional experiments may be necessary to obtain more accurate quantitative measurements of the resulting mobility. The results reported on here do, however, provide support for a model based on the use of a "mixed" mobility (or collision frequency) [26],

$$\left(\frac{1}{\omega_{ce}\tau}\right)_{\text{total}} = \left(\frac{1}{\omega_{ce}\tau}\right)_{\text{collisions}} + \left(\frac{1}{\omega_{ce}\tau}\right)_{\text{oscillations}}, \quad (9)$$

as has been originally proposed by Boeuf *et al.*, for numerical simulations of Hall discharges [7]. From Fig. 5, the Bohm value appears to be reasonable for the oscillation-induced part of the mobility, despite the lack of a full understanding of the instabilities in this region of the plasma.

While Eqn. 9 captures the general trend seen in the experimental data, it is seen in Fig. 5 that the data for the inverse Hall parameter appears to "dip" down to very low values in regions near the exit plane. This dip is strongest for the highest voltages studied. While the origin of this dip is still the subject of much debate, it is noteworthy that a similar spatial variation is seen in the "turbulence intensity" in the plasma density, as measured by the passively biased Langmuir probes. In a seminal paper by Yoshikawa and Rose [27], a statistical theory is developed relating the presence of turbulent plasma density fluctuations to the cross-field electron mobility (or inverse Hall parameter):

$$\left(\frac{1}{\omega\tau}\right)_{\text{oscillations}} = \frac{\pi}{4} \frac{\langle (n_e(t) - \bar{n}_e)^2 \rangle}{\bar{n}_e^2}. \quad (10)$$

The calculation of the inverse Hall parameter from this statistical theory is shown in Fig. 7. The resemblance between the inverse Hall parameter derived from the fluctuations in plasma density (Eqn. 10), and that from the time-average plasma properties (Fig. 6) is remarkable.

This agreement provides further support for: (i) the role played by plasma fluctuations in electron transport, and (ii) the presence of a "dip", where there appears to be a "suppression" of the turbulence, and also the reduction in the electron transport rate across the magnetic field.

## B. Azimuthal Electron Shear

While these data strongly support the association between turbulent fluctuations and anomalous electron current flow, they do not provide an explanation for the "dip" in the mobility as seen in both Fig. 6 and Fig. 7. We speculate that this suppression is at least in part attributed to the presence of a strong electron shear due to the spatially varying azimuthal drift velocity,  $v_d$ . The shear rate in the azimuthal drift velocity is:

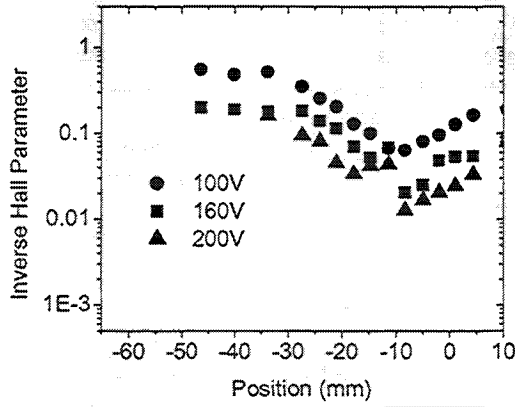


FIG. 7. Inverse Hall parameter determined from fluctuations in the electron density, and the theory of Yoshikawa and Rose [27].

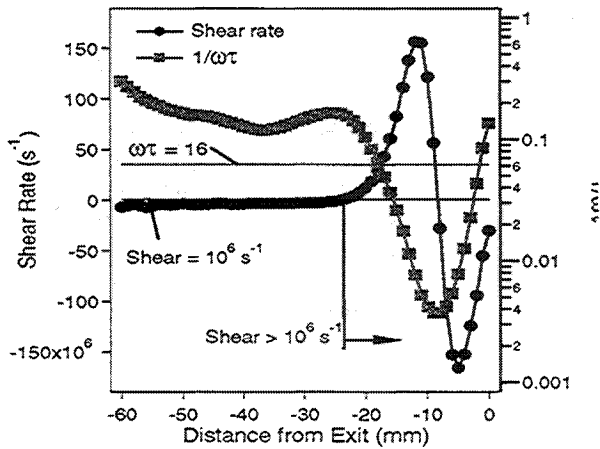


FIG. 8. Azimuthal electron shear rate, and inverse Hall parameter versus position, for a discharge voltage of 200V.

$$\alpha_\theta = \frac{\partial v_d}{\partial z} = \frac{\partial E_z / B_r}{\partial z} \quad (11)$$

A plot of the shear rate versus position within the channel, for the 200V discharge case, is shown in Fig. 8, along with the inverse Hall parameter, for comparison.

It is noteworthy that there is a correlation between the drop in the electron mobility, and the increase in the electron shear rate, ignoring the very narrow low shear region near  $z = -10$  mm (where the direction of the shear changes sign), which would be difficult to resolve in the experiments, and would likely be broadened out due to diffusion effects.

A re-analysis of the data, to plot the inverse Hall parameter versus the magnitude of the azimuthal electron shear rate (excluding the second branch which would result from the cross-over at  $z = -10$  mm, and excluding

data upstream of  $z = -25$  mm) is shown in Fig. 9. This figure includes data from all three-discharge voltages. It is noteworthy that the data collapses reasonably well onto the empirical relation:

$$\frac{1}{(\omega\tau)_{eff}} = \frac{1}{(\omega\tau)_o} \exp(1.65 \times 10^{-8} \alpha) \quad (12)$$

Here,  $1/(\omega\tau)_o \approx 0.1$  is the shear-free value, and is seen to be remarkably close to the Bohm value of  $\sim 0.06$ .

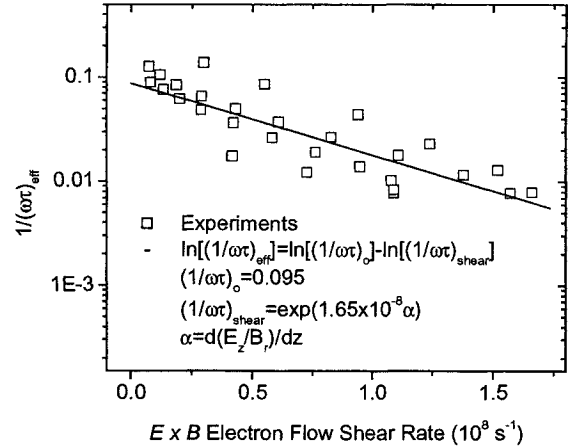


FIG. 9. Measured inverse Hall parameter versus electron shear rate, for all conditions. Note that points in the vicinity of the shear reversal ( $z = -10$  mm) have been excluded, as are values upstream of approximately  $z = -25$  mm (where the shear rate is too low to be measured accurately).

Our results therefore suggest a modified version of the transport model given in Eqn. 9, to include the possible effects of turbulence suppression due to azimuthal shear:

$$\left(\frac{1}{\omega_{ce}\tau}\right)_{total} = \left(\frac{1}{\omega_{ce}\tau}\right)_{collisions} + \left(\frac{1}{\omega_{ce}\tau}\right)_o \exp[1.65 \times 10^{-8} \alpha] \quad (12)$$

It is interesting to note that while a physical explanation for the magnitude of the exponent in Eqn. 12 is not yet available, this value of  $10^{-8}$  sec. is very close to the cyclotron period of the electron.

## V. CONCLUSIONS

A wide variety of diagnostic techniques, both intrusive and non-intrusive, have been applied to a Hall thruster to produce a consistent determination of the electron mobility. The inverse Hall parameter has been shown to approach a constant value, within the margin of

error, near the Bohm value (of  $\sim 0.06$ ) near the channel exit, in regions where probe measurements indicate a high level of turbulent fluctuations in the plasma density. The use of the statistical theory of Yoshikawa and Rose [27] which relates the inverse Hall parameter to the turbulence intensity associated with the plasma density field confirms the overall behavior in the Hall parameter derived from time averaged measurements in the plasma density. The appearance of a noticeable “dip” in the Hall parameter in regions where there is a strong spatial variation in the electron drift velocity provokes us to speculate on the possible influence that electron shear has on suppressing the turbulent fluctuations and hence mobility. An empirical model is proposed for the inverse Hall parameter based on the suppression of transport-enhancing fluctuations due to the azimuthal electron

shear. The success of this model is its ultimate ability to capture a broad range of operational characteristics when used in detailed simulations of Hall plasma thrusters.

### ACKNOWLEDGEMENTS

This work was supported by the Air Force Office of Scientific Research. Mr. Meezan was supported by a National Defense Science and Engineering Graduate (NDSEG) fellowship, and Dr. Gascon is supported in part by a fellowship provided by the European Space Agency. The authors wish to thank Dr. Eduardo Fernandez, who suggested the possibility that the shear flow may play a role in reducing the local cross-field mobility.

- 
- [1] G. S. Janes and R. S. Lowder, *Phys Fluids* **9**, 1115 (1966).
- [2] I. Morozov *et al.*, *Zh. Tekh. Fiz.* **42**, 612 (1972). [*Sov. Phys. Tech. Phys.* **17**, 482 (1972)].
- [3] Y. B. Esipchuk *et al.*, *Zh. Tekh. Fiz.* **43**, 1466 (1973).
- [4] E. Y. Choueiri, AIAA Paper No. 94-3013, *30th Joint Propulsion Conference*, Indianapolis, IN, 1994 (American Institute of Aeronautics and Astronautics, Washington, DC, 1994).
- [5] G. Guerrini and C. Michaut, *Phys. Plasmas* **6**, 343 (1999).
- [6] J. Fife and M. Martinez-Sanchez AIAA Paper No. 96-3197, *32nd Joint Propulsion Conference*, Lake Buena Vista, FL, 1996.
- [7] J. P. Boeuf and L. Garrigues (1998). “Low frequency oscillations in a stationary plasma thruster.” *J. Appl. Phys.* **84**, 3541 (1998).
- [8] J. J. Szabo, Jr. and M. Martinez-Sanchez, AIAA Paper No. 98-3795, *34th Joint Propulsion Conference*, Cleveland, OH, 1998.
- [9] E. Ahedo and M. Martinez-Sanchez, AIAA Paper No. 98-3788, *34th Joint Propulsion Conference*, Cleveland, OH, 1998.
- [10] T. Randolph *et al.*, IEPCC Paper No. 93-093, *23rd International Electric Propulsion Conference*, Seattle, WA, 1993.
- [11] S. C. Bechu *et al.*, AIAA Paper No. 99-2567, *35th Joint Propulsion Conference*, Los Angeles, CA, 1999.
- [12] W. A. Hargus, Jr. and M. A. Cappelli, AIAA Paper No. 99-2721, *35th Joint Propulsion Conference*, Los Angeles, CA, 1999.
- [13] F. F. Chen, in *Plasma Diagnostic Techniques*, edited by R. H. Huddlestone and S. L. Leonard (Academic, New York, 1965), Chap. 4, p. 184.
- [14] R. J. Cedolin, W. A. Hargus, Jr. and M. A. Cappelli, *Appl. Phys. B* **65**, 459 (1997).
- [15] A. Lieberman and A. J. Lichtenberg., *Principles of Plasma Discharges and Materials Processing* (Wiley, New York, 1994) p.174.
- [16] G. S. Janes and J. P. Dotson, *Rev. Sci. Instr.* **8**, 284 (1964).
- [17] M. Bishaev and V. Kim, *Zh. Tekh. Fiz.* **48**, 1853 (1978) [*Sov. Phys. Tech. Phys.* **23**, 1055 (1978)].
- [18] I. Bugrova *et al.*, *Teplofiz. Vys. Temp.* **19**, 1149 (1981).
- [19] CPAT and Kinema Software, [www.csn.net/siglo](http://www.csn.net/siglo) (1998).
- [20] D. Bohm in *The characteristics of electrical discharges in magnetic fields*, edited by A. Guthrie and R.K. Wakerling, (McGraw, New York, 1949), Chap. 2, p. 65
- [21] N. B. Meezan and M. A. Cappelli, AIAA Paper No. 99-2284, *35th Joint Propulsion Conference*, Los Angeles, CA, 1999.
- [22] D. P. Schmidt, N. B. Meezan, and M. A. Cappelli, AIAA Paper No. 99-3437, *30th Plasmadynamics and Lasers Conference*, Norfolk, VA, 1999.
- [23] E. Chesta, C. Lam, N.B. Meezan, and M.A. Cappelli, *IEEE Transactions in Plasma Science*, submitted, 2000.
- [24] D. Pagnon *et al.*, AIAA Paper No. 99-2428, *35th Joint Propulsion Conference*, Los Angeles, CA, 1999.
- [25] D. Kusamoto and K. Komurasaki, IEPCC Paper No. 97-067, *25th International Electric Propulsion Conference*, Cleveland, OH, 1997.
- [26] N.B. Meezan, W.A. Hargus, Jr., and M.A. Cappelli, *Phys. Rev. E* **63**, 026410, 2001.
- [27] S. Yoshikawa and D.J. Rose, *Phys. Fluids* **5**, 334 (1962).